

PHYSICAL REVIEW B

CONDENSED MATTER

THIRD SERIES, VOLUME 46, NUMBER 3

15 JULY 1992-I

Quantum oscillations from the cylindrical Fermi-surface sheet of potassium created by the charge-density wave

Graciela Lacueva

Department of Physics, John Carroll University, University Heights, Ohio 44118

A. W. Overhauser

Department of Physics, Purdue University, West Lafayette, Indiana 47907

(Received 6 February 1991)

Oscillations reported by Dunifer *et al.* in microwave transmission through thin K layers are found to be periodic in $1/H$. The oscillations arise from conduction-electron Landau levels passing through a small cylindrical sheet of the Fermi surface. This cylinder had been envisioned theoretically after incorporating both charge-density-wave and crystalline potentials in Schrödinger's equation. The cylinder's cross-sectional area is found to be $\pi k_F^2/69$, in agreement with the area inferred from the perpendicular-field cyclotron resonance, discovered by Grimes in the surface impedance.

Microwave transmission through thin K layers in a magnetic field H perpendicular to the surface reveals several signals having no conventional explanation.¹ One of these surprising phenomena—the high-frequency oscillation—was seen in nine samples and is the focus of this work. The periodicity turns out to be linear in $1/H$, which is the signature of Landau-level oscillations, but their frequency is 69 times smaller than the well-known de Haas–van Alphen value.

Data from sample K-4, which had the longest and clearest sequence, are shown in Fig. 1. The conduction-electron spin resonance (together with associated spin-wave sidebands) and the Gantmakher-Kaner oscillations have been understood for many years. The source of the new Landau-level oscillations, as will be explained below, is a small cylindrical sheet of Fermi surface created by the charge-density-wave (CDW) broken symmetry.² This cylinder, which contains only a fraction $\eta=4 \times 10^{-4}$ of the conduction electrons, is also responsible for the dramatic cyclotron resonance near $\omega_c/\omega=1$ in Fig. 1.³

Before discussing the origin and geometry of the Fermi-surface cylinder, we shall analyze the data of Fig. 1, for which the horizontal axis, linear in H , is $x = \omega_c/\omega$, where ω_c is the Azbel-Kaner cyclotron frequency and $\omega/2\pi$ is the microwave frequency. $\omega_c = eH/m^*c$. For K, $m^*/m = 1.21$.⁴ Twelve complete oscillations are rather well defined within the two vertical lines of Fig. 1. The ω_c/ω coordinates of the maxima and minima are

given in Table I. (These values apply only for the microwave frequency $f = 79.18$ GHz.) At first glance the oscillations appear to be periodic in x , but we shall test this supposition by finding the best discrete sequence,

$$x_n = sn + b, \quad (1)$$

which fits the 12 maxima (or minima). The values of s and b that minimize the mean-square deviation,

$$D = \frac{1}{12} \sum_{n=1}^{12} [X_n - (sn + b)]^2, \quad (2)$$

TABLE I. ω_c/ω values, X_n , for the maxima and minima of the signal shown in Fig. 1.

| n | Maxima | Minima |
|-----|--------|--------|
| 1 | 1.085 | 1.090 |
| 2 | 1.098 | 1.105 |
| 3 | 1.112 | 1.121 |
| 4 | 1.128 | 1.137 |
| 5 | 1.146 | 1.154 |
| 6 | 1.163 | 1.173 |
| 7 | 1.181 | 1.190 |
| 8 | 1.202 | 1.210 |
| 9 | 1.220 | 1.230 |
| 10 | 1.238 | 1.249 |
| 11 | 1.259 | 1.267 |
| 12 | 1.277 | 1.286 |

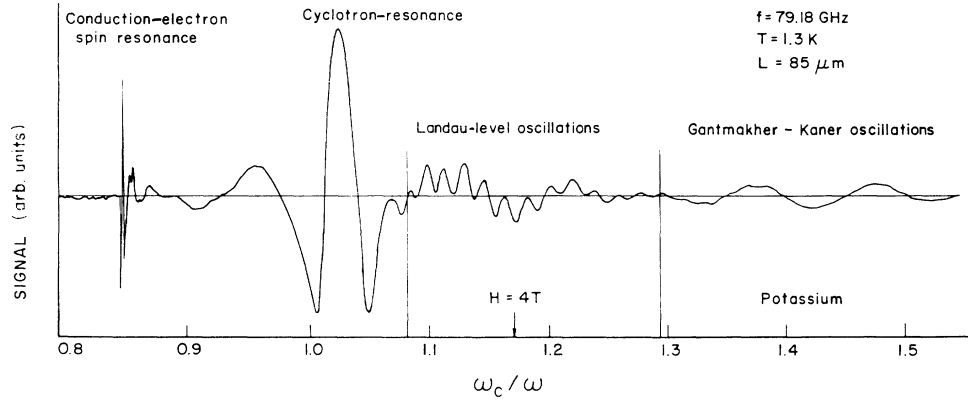


FIG. 1. Microwave transmission signal vs H through a K plate in a perpendicular magnetic field. $H = 3.42$ T at $\omega_c/\omega = 1$. The phase of the microwave reference was adjusted so that the cyclotron resonance was symmetric. The data displayed on this figure were provided by G. L. Dunifer (unpublished).

are $s = 1.779 \times 10^{-2}$, $b = 1.060$ for the maxima and $s = 1.804 \times 10^{-2}$, $b = 1.067$ for the minima. The mean-square fractional deviation, $D/(X_6)^2$, is 7.9×10^{-6} for the maxima and 4.4×10^{-6} for the minima.

The foregoing fit should be compared to one obtained by supposing the periodicity to be linear in $1/H$. We then seek the best sequence,

$$\frac{1}{x_n} = b' - s'n. \quad (3)$$

The mean-square deviation to be minimized is now

$$D' = \frac{1}{12} \sum_{n=1}^{12} \left[\frac{1}{X_n} - (b' - s'n) \right]^2. \quad (4)$$

The solutions are $s' = 1.287 \times 10^{-2}$, $b' = 0.936$ and $s' = 1.288 \times 10^{-2}$, $b' = 0.930$ for maxima and minima, respectively. The mean-square fractional deviations, $D'(X_6)^2$, are 1.54×10^{-6} and 9.8×10^{-7} . Observe that these χ^2 fitting errors are much smaller, by factors of 5.1 and 4.5, respectively, than those obtained with the linear sequence, Eq. (1). A detailed analysis of χ^2 versus the periodicity power is given below. It was reported that the periodicity did not depend on sample thickness. Accordingly, we conclude that the high-frequency oscillations are best described by periodicity in $1/H$, and so arise from Landau levels passing through an appropriate sheet of the conduction-electron Fermi surface.

Landau-level quantization causes periodic variation of any physical property that depends on conduction-electron response.⁵ A property y will then acquire an oscillatory component,

$$\Delta y \sim \cos \left[\frac{2\pi F}{H} + \phi \right], \quad (5)$$

where F is the de Haas-van Alphen frequency,

$$F = \frac{\hbar c A}{2\pi e}. \quad (6)$$

A is the external area in k space (perpendicular to \mathbf{H}) of the Fermi surface involved. For K, with lattice constant $a = 5.2295$ Å at 4.2 K, a free-electron Fermi sphere has $A_0 = \pi k_F^2$ and $F_0 = 1.828 \times 10^4$ T. ($k_F = 7.45 \times 10^7$ cm⁻¹.)

The frequency F_c that describes the oscillations in Fig. 1 is H_0/s' , where H_0 is the magnetic field corresponding to $\omega_c/\omega = 1$. $\omega/2\pi = 79.18$ GHz, so we obtain $H_0 = 3.42$ T and

$$F_c = 266 \text{ T}. \quad (7)$$

If πk_c^2 is the cross section of the Fermi surface causing these oscillations, then

$$\frac{k_F^2}{k_c^2} = \frac{F_0}{F_c} = 69. \quad (8)$$

We now turn our attention to the microscopic origin of the small Fermi-surface structure which explains the ratio (8).

The CDW wave vector \mathbf{Q} in K has been measured by neutron diffraction,⁶ and identification of the satellites as CDW structure was recently confirmed⁷ (Ref. 7 reviews other data, too):

$$\mathbf{Q} = (0.995, 0.975, 0.015) \times \frac{2\pi}{a}, \quad (9)$$

which differs from the \mathbf{G}_{110} reciprocal-lattice vector by 2%. Electronic band structure near $\frac{1}{2}\mathbf{Q}$ was studied by solving Schrödinger's equation having both a CDW potential and a lattice potential:⁸

$$V(\mathbf{r}) = 2\alpha \cos(\mathbf{Q} \cdot \mathbf{r}) + 2\beta \cos(\mathbf{G}_{110} \cdot \mathbf{r}). \quad (10)$$

A family of higher-order "minigaps" appears in the region near $\pm \frac{1}{2}\mathbf{Q}$. These new gaps will introduce infrared structure in the optical properties,⁹ and recent work using the inverse photoelectric effect attributes infrared-emission peaks in Li (Ref. 10) and in Na and K (Ref. 11)

to these minigaps.

The effect of the CDW on K's Fermi surface was studied¹² after Q was measured. One or more small cylindrical sheets of Fermi surface are generated by the minigap structure. The axis of each cylinder is parallel to $Q' \equiv G_{110} - Q$. One such cylinder is shown in Fig. 2, and consists of two half-cylinders pieced together by Bragg reflections having the relevant periodicity. The angle between Q' and [110] is $\sim 44^\circ$, but the cross section is approximately circular in a plane perpendicular to [110]. The length of the cylinder is $|Q'|$, but its height (parallel to [110]) is

$$\delta = 0.015 \times \sqrt{2} \left(\frac{2\pi}{a} \right). \quad (11)$$

If k_c is the cylinder radius (in the plane perpendicular to [110]), then the volume (including both halves) is

$$\Omega = \pi k_c^2 \delta. \quad (12)$$

The fractional number η of conduction electrons within the cylinder is, of course,

$$\eta = 3\Omega / 4\pi k_F^3. \quad (13)$$

Four years ago we found¹³ that an unexpected cyclotron resonance in the perpendicular-field surface impedance¹⁴ could be explained if a small Fermi-surface

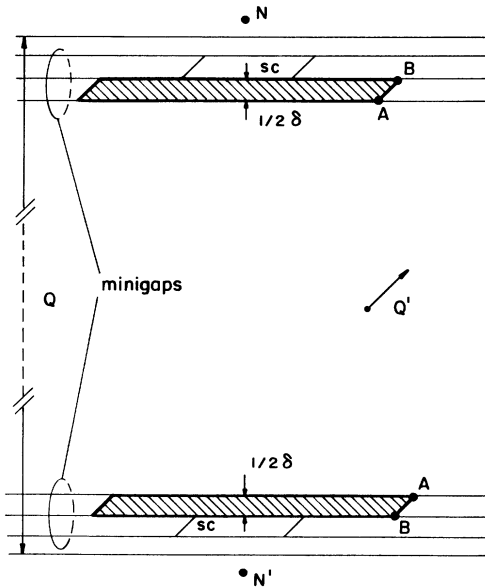


FIG. 2. Schematic drawing of a Fermi-surface cylinder formed by two CDW minigaps. The two shaded half-cylinders can be joined because the A points are the same quantum state, and so are the B points. (Two points in \mathbf{k} space can be equivalent if they differ by $Q - nQ'$.) There is evidence that indicates the existence of a smaller cylinder (sc) in the adjacent minigap region. For theoretical details see Ref. 12. The points N and N' are the centers of the two Brillouin-zone faces (on opposite sides of the Fermi surface). 99.96% of the occupied volume within the Fermi surface, i.e., the region bounded (in part) by the planes through the A points, is not shown.

cylinder was included in the theory. The \mathbf{k} -space volume of the cylinder was determined by the size of the anomaly relative to the change in surface impedance between $H = 0$ and H at resonance. The value of η needed was

$$\eta = 4 \times 10^{-4}. \quad (14)$$

Despite this small value, the cylinder accounts for 2% of the density of states at the Fermi energy. Equations (12)–(14) provide an independent determination of the cylinder's radius:

$$\frac{k_F^2}{k_c^2} = 64. \quad (15)$$

The agreement between (8), derived from Landau-level quantization, and (15), derived from semiclassical magnetotransport, is remarkable.

The small value of $k_c \sim k_F/8$ solves a puzzle that can be noticed in Grime's data. The sharpness of the resonance requires $\omega_c \tau \sim 60$, whereas the measured bulk resistivity (at 2.5 K) would yield $\omega_c \tau \sim 10$. The longer relaxation time, τ , by a factor ~ 6 , for the cylinder electrons can be understood, since their velocity is approximately six times smaller than v_F . Consequently, they encounter scattering centers at a reduced rate. A similar factor (i.e., ~ 3) is also necessary to reconcile the sharpness of the cyclotron resonance seen in microwave transmission. (Without the cylinder the resonance should not even occur.)

There are now five phenomena that require a small Fermi-surface cylinder in K.

(i) The cyclotron resonance in the perpendicular-field surface impedance.¹³

(ii) The cyclotron resonance in the perpendicular-field microwave transmission.³

(iii) The Landau-level oscillations in the microwave transmission.

(iv) Subharmonic cyclotron resonance, i.e., at $H_0/2$, $H_0/3$, etc., in the microwave transmission. This phenomenon was found in 14 samples.¹ The angular tilt of the cylinder axis by $\sim 44^\circ$ causes the elliptical orbits in *real space* to be tilted by 44° . The resulting electron vibrations parallel to H lead to subharmonic coupling (as in the Azbel-Kaner effect) even though H is perpendicular to the surface.

(v) A sharp (angle-resolved) photoemission peak originating from electron states near the Fermi level and at photon energies for which no emission should occur. This phenomenon has been observed in Na (Ref. 15) and K.¹⁶ The sharp Fermi-energy peak is caused by electrons that (before excitation) occupy the cylinder.¹⁷ The sharpness results from the fact that $E(\mathbf{k})$ is flat along the cylinder axis, unlike the steep E versus $|\mathbf{k}|$ that would otherwise occur near E_F . Photoexcitation of the cylinder electrons is ubiquitous because a cylinder wave function $|\mathbf{k}\rangle$ includes many other components, e.g., $|\mathbf{k} \pm n\mathbf{G}'\rangle$.

The common feature of these five striking experimental discoveries is that they all occur in thin samples which may be expected to have epitaxial texture as a result of adhesion to a smooth surface. This causes a [110] axis to be perpendicular to the sample face.¹⁸ Q is tilted only

0.8° from [110]. Each crystallite can have one of four Q' directions: (0.025,0.005,±0.015) or (0.005,0.025,±0.015). When all crystallites are considered, the cylinder axes will be randomly distributed on a cone having a 44° angle with [110], the surface normal. Nevertheless all cross-sectional areas perpendicular to H (and to [110]) and all cyclotron masses would be the same. Naturally, imperfect epitaxial texture will lead instead to an unpredictable distribution in cyclotron mass or extremal area. One should then expect to find structure in the cyclotron resonance, and the field range of the Landau-level oscillations will be limited. These features do indeed occur and vary from sample to sample.¹ (Such effects cannot be attributed to a martensitic transformation, since a new low-temperature phase does not occur in K.)

There are many other phenomena that reveal the complex structure of K's Fermi surface, caused by the CDW.¹⁹ The relevance of the nearly isotropic de Haas–van Alphen effect is, however, frequently interposed. A typical specimen is a mm-size sphere or cylinder that has *not* been etched. Q-domain sizes are likely too small to allow coherent CDW effects in magnetic quantization.²⁰ Furthermore, the cylinder axes in a single crystal would have 24 possible orientations. One should not be surprised, then, if the Landau-level oscillations from the cylinders were obscured by a lack of orientational uniformity. The quantum oscillations in microwave transmissions show that de Haas–van Alphen studies of K have been incomplete and misleading.

Finally, we search for the periodicity exponent p that best fits the transmission peaks of Table I. (The inquiry above involved only $p = 1$ or -1 , values that have physical interpretations.) Suppose the oscillations were described by

$$\Delta y \sim \cos(\lambda H^p + \phi), \quad (16)$$

instead of by Eq. (5). The parameters λ and ϕ , which optimize the fit, were found for all values of p , and the peak locations $x_n(p)$ were computed. The mean-square deviations from the observed peaks X_n are shown in Fig. 3. The optimum fit occurs for $p = -1.0$, the precise value appropriate for Landau-level oscillations.

Landau-level oscillations observed by a de Haas–van Alphen effect increase in amplitude with increasing field. However, such monotonic behavior should *not* occur for microwave transmission. These oscillations arise from a

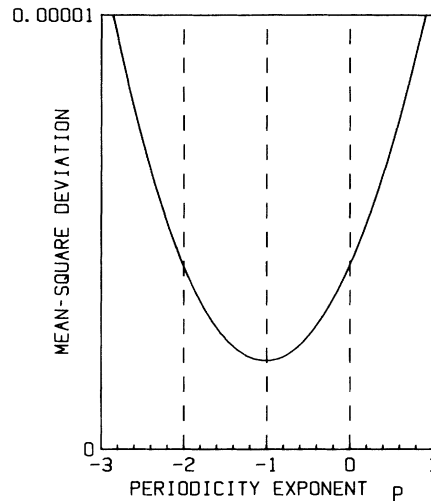


FIG. 3. Mean-square deviation $[X_n - x_n(p)]_{av}^2$ vs p , the periodicity exponent in Eq. (16).

periodic variation in the scattering rate $1/\tau$ (caused by an oscillation in the Fermi-surface density of states). An easy exercise to see how τ affects microwave transmission (parallel to a magnetic field) is to calculate the propagation constant q (starting from Maxwell's curl H equation). The result for conduction electrons, in a local approximation, is

$$q = \left[\frac{4\pi i (ne^2\tau/m)/c^2}{1 + i(\omega_c - \omega)\tau} \right]^{1/2}. \quad (17)$$

($ne^2\tau/m$ is the dc conductivity.) Observe that when $(\omega_c - \omega)\tau$ is near zero (i.e., not far from cyclotron resonance), q depends on τ . Consequently, the transmitted signal will have oscillations. However, when $(\omega_c - \omega)\tau \gg 1$, the τ 's in the numerator and denominator of (17) cancel. Accordingly, q no longer depends on τ , so the Landau-level transmission oscillations will disappear at high magnetic fields, as exhibited by the data in Fig. 1.

We are grateful to the National Science Foundation, Condensed-Matter Theory Program for financial support. We especially thank G. L. Dunifer for providing the data shown in Fig. 1.

¹G. L. Dunifer, J. F. Sambles, and D. A. H. Mace, *J. Phys. Condens. Matter* **1**, 875 (1989).

²A. W. Overhauser, *Adv. Phys.* **27**, 343 (1978).

³Graciela Lacueva and A. W. Overhauser (unpublished).

⁴C. C. Grimes and A. F. Kip, *Phys. Rev.* **132**, 1991 (1963).

⁵D. Shoenberg, *Magnetic Oscillations in Metals* (Cambridge University Press, London, 1984), Chap. 4.

⁶T. M. Giebultowicz, A. W. Overhauser, and S. A. Werner, *Phys. Rev. Lett.* **56**, 2228 (1986).

⁷S. A. Werner, A. W. Overhauser, and T. M. Giebultowicz, *Phys. Rev. B* **41**, 12 536 (1990).

⁸F. E. Fragachán and A. W. Overhauser, *Phys. Rev. B* **29**, 2912

(1984).

⁹F. E. Fragachán and A. W. Overhauser, *Phys. Rev. B* **31**, 4802 (1985).

¹⁰Yu. M. Kobzar', N. N. Bodnar, V. Ya. Kozych, and V. G. Kovtun, *Pis'ma Zh. Eksp. Teor. Fiz.* **50**, 323 (1989) [*JETP Lett.* **50**, 358 (1989)].

¹¹Yu. M. Kobzar' and N. N. Bodnar, *Pis'ma Zh. Eksp. Teor. Fiz.* **52**, 686 (1990) [*JETP Lett.* **52**, 37 (1990)].

¹²Yong Gyo Hwang and A. W. Overhauser, *Phys. Rev. B* **39**, 3037 (1989).

¹³G. Lacueva and A. W. Overhauser, *Phys. Rev. B* **33**, 3765 (1986).

- ¹⁴G. A. Baraff, C. C. Grimes, and P. M. Platzman, *Phys. Rev. Lett.* **22**, 590 (1969).
- ¹⁵E. Jensen and E. W. Plummer, *Phys. Rev. Lett.* **55**, 1912 (1985).
- ¹⁶B. S. Itchkawitz, In-Whan Lyo, and E. W. Plummer, *Phys. Rev. B* **41**, 8075 (1990).
- ¹⁷A. W. Overhauser, *Phys. Rev. Lett.* **55**, 1916 (1985); **58**, 959 (1987).
- ¹⁸A. W. Overhauser and N. R. Butler, *Phys. Rev. B* **14**, 3371 (1976).
- ¹⁹A. W. Overhauser, in *Highlights of Condensed-Matter Theory, Proceedings of the International School of Physics "Enrico Fermi,"* Course LXXXIX, Varenna on Lake Como, 1983, edited by F. Bassani, F. Fumi, and M. P. Tosi (North-Holland, Amsterdam, 1985), p. 194.
- ²⁰A. W. Overhauser, *Can. J. Phys.* **60**, 687 (1982).